Cement and Concrete Research 40 (2010) 1157–1164

Contents lists available at ScienceDirect

Cement and Concrete Research

journal homepage: http://ees.elsevier.com/CEMCON/default.asp

Biologically induced concrete deterioration in a wastewater treatment plant assessed by combining microstructural analysis with thermodynamic modeling

A. Leemann *, B. Lothenbach, C. Hoffmann

Empa, Dübendorf, Switzerland

ARTICLE INFO

Article history:
Received 12 October 2009
Accepted 10 March 2010

Keywords:
Durability (C)
Acid attack
Microstructure (B)
Thermodynamic modeling (E)

ABSTRACT

In the nitrification basins of wastewater treatment plants, deterioration of the concrete surface can occur due to acid attack caused by a nitrifying biofilm covering the concrete.
To identify the mechanism of deterioration, concrete cubes of different composition were suspended in an aerated nitrification basin of a wastewater treatment plant for two years and analyzed afterwards.
The microstructural investigation reveals that not only dissolution of hydrates takes place, but that calcite precipitation close to the surface occurs leading to the formation of a dense layer. The degree of deterioration of the different cubes correlates with the CaO content of the different cements used. Cements which contain a high fraction of CaO form more calcite offering a better protection against the acid attack. The presence of slag, which lowers the amount CaO in the cement, leads to a faster deterioration of the concrete than observed for samples produced with pure OPC.

1. Introduction

Biologically induced concrete deterioration can be observed in a variety of environments (e.g. [1–3]). One of them is wastewater transport and treatment. Attack in sewer pipes usually takes place due to H_2S production of sulphate reducing bacteria and the subsequent formation of sulphuric acid by sulphate oxidizing bacteria (e.g. [1,4–6]). But concrete deterioration is not limited to the occurrence of biological processes involving sulphur. In wastewater treatment plants, where aerobic conditions prevail, deterioration of the concrete surface can be observed in aerated nitrification basins. The bacteria present as suspension in the wastewater and as a biofilm on the concrete surface oxidize ammonium to form nitrate (Eqs. (1) and (2)):

$$NH_3 + 1.5\ O_2 \rightarrow NO_2^- + H_2O + H^+ \quad (1)$$

$$NO_2^- + 0.5\ O_2 \rightarrow NO_3^- \quad (2)$$

These reactions cause a decrease of pH due to proton formation (see Eqs. (1) and (2)) [7,8] and lead to an acid attack on the biofilm covered concrete surface. The pH decrease in the biofilm is about 0.1. [9]. The biologically induced attack leads to a deterioration of the concrete surface, which decreases the thickness of the concrete cover protecting the reinforcement and with it the durability of the structure. In addition, sand and gravel from the degraded concrete falling to the floor of the basins have to be removed periodically, as pumps can be damaged by eroded concrete aggregates.

In an attack by slightly acid liquids or water undersaturated in calcium carbonate, hydration products of cementitious systems are dissolved in the order of portlandite, AFm, AFt, calcite and, progressively, C–S–H decalcification [10–12] leading to the formation of a silica-rich layer at the surface. The transport of attacking solution and dissolved ions is a function of diffusion and the dissolution front progresses with the square root of time [12–15]. Consequently, the progress of the dissolution front slows down with time. There are several additional factors influencing its progress. Firstly, the formation and preservation of the silica-rich layer at the surface is crucial. When it is removed due to physical action like strong currents or brushing, the rate of dissolution increases to the initial level and total leaching is accelerated [16–18]. Secondly, the rate of dissolution is decreased with decreasing water-to-cement ratio (w/c) due to decreased porosity and diffusivity [19–21]. Thirdly, the type of binder has an influence on the diffusion coefficient. Systems with slag or fly ash have shown more resistance to leaching than systems with ordinary Portland cement [12,20,22].

Numerous studies deal with nitrifying bacteria present in wastewater (e.g. [23–25]). However, there is little knowledge on the microstructural and chemical consequences for concrete exposed to a nitrifying biofilm.

In this project, the mechanisms of concrete deterioration are studied by exposing concrete cubes in a wastewater plant. In order to study only the influence of cement composition, aggregate composition and water-to-cement ratio (w/c), as two parameters very probably influencing concrete deterioration as well, were kept

* Corresponding author.
E-mail address: andreas.leemann@empa.ch (A. Leemann).

0008-8846/$ – see front matter © 2010 Elsevier Ltd. All rights reserved.
doi:10.1016/j.cemconres.2010.03.007

constant. Concrete mixtures produced with four different cements were used. After an exposure of two years, the concrete cubes were recovered. The oxygen diffusion coefficient of the unaffected inner part of the cubes was measured. Degree of deterioration of the concrete surface was assessed by analyzing microstructure and chemical composition. The experimental data were completed by thermodynamic modeling of the changes induced in concretes by the presence of slightly acid solutions containing bicarbonates.

2. Materials and methods

2.1. Experiments

Four cements with different composition were used to produce the concrete mixtures and cubes (dimensions of 200×200×200 mm; Tables 1 and 2); CEM I contains up to 5% limestone filler, CEM II/A-LL up to 20% limestone filler, CEM II/A-S up to 20% slag and CEM III/B up to 80% slag. A water-to-cement ratio (w/c) of 0.50 was used. The concrete was produced with alluvial sand and gravel consisting of sandstone, limestone and minor amounts of igneous/metamorphic rocks (grain size distribution of 0–32 mm). The superplasticizer used was based on naphthalene sulphonate.

A waste water plant showing problems of concrete deterioration was selected to expose the cubes. Water hardness in the plant fluctuates between 17 and 22 fH°, while pH values are kept at 7 adding alkaline solutions. This value is required to ensure the stability of the microorganisms and with it an effective nitrification. After reaching an age of 90 days, the cubes were immersed in an aerated nitrification basin. They were suspended at a depth of 5.0 m (1.2 m above the floor) using outriggers. After two years, the exposure was terminated and the cubes were investigated in the laboratory.

Oxygen diffusion was determined on two cores (diameter of 100 mm, length of 20 mm) taken from the inner part of the cubes unaffected by acid attack. The cores were first dried at 50 °C for seven days and then at 110 °C for two days. On one side of the core an oxygen flow was applied and on the other side a nitrogen flow, both having identical pressure. The oxygen content in the nitrogen flow was measured until equilibrium was reached. Afterwards, the oxygen diffusion coefficient was calculated according to Lawrence [26].

Cores of the surface (diameter of 50 mm) were used for the microstructural investigation. The samples were dried in an oven at 50 °C for three days, impregnated with epoxy resin and polished. In a first step, the samples were studied with an optical microscope. A reconstruction of the position of the original surface was made possible as parts of it were not eroded and were preserved during sample preparation as well. At 10 different locations per cube, the different layers formed due to deterioration where identified and their depth was measured perpendicular to the concrete surface. For further investigation of the samples, an environmental scanning electron microscope (ESEM-FEG XL30) was used. The carbon coated samples were studied in the high vacuum mode ($2.0–6.0 \cdot 10^{-6}$ Torr) with an accelerating voltage of 15 kV and a beam current of 275–280 μA.

Layers of different porosity were defined. The software for segmentation of the phases was developed in Matlab. The pixel size of the images used for the analysis was 1.55×1.72 μm^2. Consequently, the resolution was not sufficient to resolve gel or capillary pores. Hence, the segmented "porosity" represent porous zones in the paste.

Table 2
Mix design of the concrete.

Mixture	C-OPC	C-LS	C-SL-1	C-SL-2
Cement type	CEM I 42.5 N	CEM II/A-LL 42.5 N	CEM II/A-S 32.5 R	CEM III/B 32.5 R
Cement content [kg/m^3]	325	325	325	325
Aggregate 0/32 mm [kg/m^3]	1940	1935	1935	1920
Water [kg/m^3]	163	163	163	163
Superplasticizer [kg/m^3]	3.25	3.25	3.25	3.25
w/c	0.50	0.50	0.50	0.50

The porosity was analyzed in bands with a width of 15.5 μm as a function of depth. The determined values are relative and can be used to compare the porosity of the different layers. They are not comparable to porosity analyzed with other methods like mercury intrusion porosimetry or thermodynamic modeling.

The chemical composition of the concrete's surface layers was determined with energy dispersive X-ray spectroscopy (EDX). An EDAX 194 UTW detector, a Philips digital controller and Genesis Spectrum Software (Version 4.6.1) with ZAF corrections were used. In each layer ten area scans (about 20×20 μm^2) of the "outer product" were made to analyze its chemical composition. The area scans were selected to avoid aggregates.

2.2. Thermodynamic modeling

Thermodynamic modeling was used to study the chemical changes associated with the ingress of carbonate containing solutions in the different cement types. Thermodynamic modeling was carried out using the Gibbs free energy minimization program GEMS [27]. GEMS is a broad-purpose geochemical modeling code which computes equilibrium phase assemblage and speciation in a complex chemical system from its total bulk elemental composition. Chemical interactions involving solids, solid solutions, and aqueous electrolytes are considered simultaneously. The speciation of the dissolved species as well as the kind and amount of solids precipitated is calculated.

The thermodynamic data for aqueous species as well as for many solids were taken from the PSI-GEMS thermodynamic database [28,29]. Solubility products for cement minerals including ettringite, different AFm phases, hydrogarnet, C–S–H and hydrotalcite were taken from the recent cemdata07 compilation [30]. For C–S–H an ideal solid solution between a jennite and a tobermorite type C–S–H was used, but no solid solution between tobermorite and amorphous SiO_2. For the calculations it was assumed that all of the Portland cement had reacted, but only 50% of the slag (85 mass%) present in the CEMIII/B, as a significant fraction of the slag is expected to remain unhydrated. Escalante et al. [31] found a degree of reaction of 20–50% for slag blended with OPC, depending on hydration temperature, w/b ratio and replacement level. Lumley et al. [32] reported for slags blended with Portland cement degrees of hydration between 30–55% after 28 days and 45–75% after 1–2 years. In the calculations the dissolution of amorphous SiO_2 gel was prevented as its dissolution kinetics is very slow at neutral and slightly alkaline pH conditions [33,34].

The composition of waste water can be highly variable. Besides solid particles and organic compounds it may also contain dissolved inorganic ions such as nitrate, sulphate, bicarbonate, chloride, calcium, magnesium, sodium, and potassium as well as other elements. As no detailed

Table 1
Composition of the four cements (n.a. = not analyzed).

Type	CaO [%]	SiO_2 [%]	Al_2O_3 [%]	Fe_2O_3 [%]	MgO [%]	K_2O [%]	Na_2O [%]	SO_3 [%]	CO_2 [%]	Blaine [cm^2/g]	Loss on ignition [%]	Density [kg/m^3]
CEM I 42.5 N	62.8	19.7	4.6	2.8	1.9	0.98	0.16	3.1	1.5	2940	2.8	3.13
CEM II/A-LL 42.5 N	61.3	17.4	4.1	2.5	1.7	0.84	0.12	2.8	5.7	3850	7.5	3.07
CEM II/A-S 32.5 R	57.3	22.9	5.6	2.5	2.7	0.99	0.27	3.0	n.a.	3320	1.6	3.09
CEM III/B 32.5 N	47.8	31.6	9.6	1.7	4.9	0.60	0.30	2.8	0.6	5360	1.9	2.94

Table 3
Oxygen diffusion of the four concrete mixtures.

Concrete	C-OPC	C-LS	C-SL-1	C-SL-2
O_2-diffusion coefficient [10^{-8} m^2/s]	1.10	1.68	0.82	0.38

information of the changes of these elements with time were available and as its high variability would have made it very difficult to define meaningful average values, the composition of the waste water was strongly simplified. The presence of in total 2 mmol/l CO_3^{2-} was taken into account in the thermodynamic calculations, corresponding to the 20 fH° reported in the waste water treatment plant. The carbonate was assumed be present as 0.67 mmol/l $CaCO_3$ and 1.33 mmol/l H_2CO_3 to be consistent with the pH value of 7, which was maintained in the waste water.

However, additional calculations were carried out to check the validity of this simplified approach including the presence of 1 mmol/l sodium, magnesium, sulphate and nitrate. Their presence had a small effect on the amount and kind of solids calculated. The conditions inside the biofilm were also tried to be mimicked assuming additionally the presence of 1.2 mmol/l HNO_3 resulting in a pH of 5.4, a value below the expected pH in a nitrifying biofilm [9]. The consideration of HNO_3 resulted in a slightly higher leaching of the surface and in a reduction of the amount of precipitated calcite.

Thermodynamic modeling can be used to calculate the changes associated with the ingress of carbonate or acid in a concrete sample. The ingress of carbonates can be mimicked in these calculations assuming that the core of the sample is in contact with no additional solution containing carbonates, while the area near the surface is in contact with large quantities of solution. Even though these calculations do not relate directly to time and space, it is a convenient way to calculate the different conditions that a concrete sample submersed in carbonate solutions experiences. Such a modeling approach has the advantage that the calculations are very fast and flexible as no transport equations have to be considered, but has the disadvantage that the calculated data relate neither to time nor to distance.

3. Results

3.1. Oxygen diffusion coefficient

The oxygen diffusion coefficient of the different concrete mixtures varies significantly. Concrete C-SL-2 with slag shows the lowest value and concrete C-LS with limestone the highest (Table 3).

3.2. Porosity

Qualitatively, all four concrete mixtures show the same distribution of porosity close to the surface (Fig. 1). There is a transition from the unaltered paste to a layer of increased porosity with a thickness between 100 and 800 μm. The subsequent layer is very dense and only between 10 and 40 μm thick. Finally, there is a layer of high porosity with a thickness between 100 and 700 μm at the surface of the concrete. All these layers are formed in the concrete. The segmentation of the images and their analysis show these differences in porosity more clearly (Figs. 2 and 3). According to the differences in porosity, four layers can be identified:

- layer C: core, unaltered paste
- layer IP: inner layer with increased porosity compared to the unaltered paste
- layer HD: thin layer with high density
- layer OP: outer leached layer at the surface of the concrete with high porosity.

The distance of these layers to the original uncorroded surface varies depending on concrete composition (Table 4). Within a specific concrete, these distances vary within a certain range. As an example, the standard deviation of the depth of layer HD in concrete C-OPC is ±0.12 mm (10 measured points).

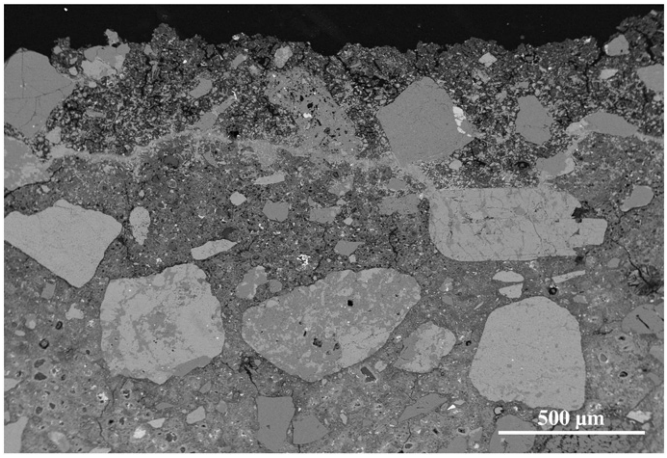

Fig. 1. Cut perpendicular to the surface of concrete C-OPC. Backscattering electron image.

3.3. Chemical composition

The depth profiles of chemical composition are directly related to the ones of porosity and are very similar for all concrete mixtures.

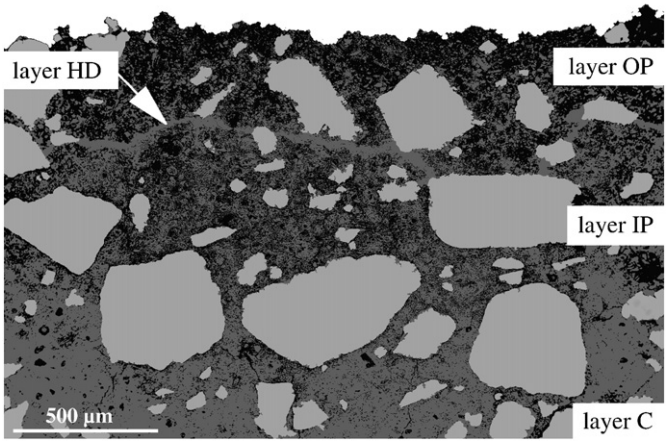

Fig. 2. Segmentation of Fig. 1 into three classes: aggregates (light grey), paste (dark grey) and pores (black). Identification of four layers based on their porosity.

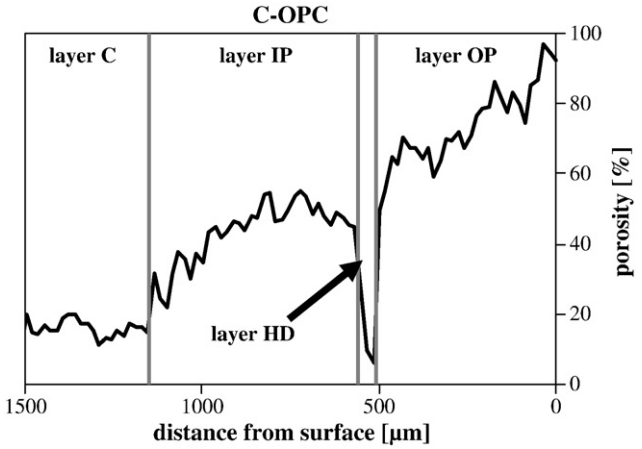

Fig. 3. Porosity distribution of the paste at the surface of concrete C-OPC as analyzed from Figs. 1 and 2. Mean values for depth and porosity are given in Table 4.

Table 4
Mean values for depth and porosity of the surface layers. The standard deviation of the depth of layer HD is between 100 and 200 µm.

Concrete	C-OPC	C-LS	C-SL-1	C-SL-2
Depth layer C [µm]	>1900	>1550	>1800	>2900
Depth layer IP [µm]	1050–1900	1000–1550	1200–1800	1450–2900
Depth layer HD [µm]	1000–1050	950–1000	1150–1200	1400–1450
Depth layer OP [µm]	<1000	<950	<1150	<1400
Porosity layer C [%]	16	20	19	18
Porosity layer IP [%]	39	35	43	30
Porosity layer HD [%]	8	6	9	12
Porosity layer OP [%]	73	80	83	79

Layer IP shows a depletion of Ca compared to the unaltered paste. Apparently, it is leached from portlandite and C–S–H. The Ca concentration in the paste decreases from 55% to 40% in layer IP. The main component of layer HD is Ca that is present as calcite aggregations with a diameter of several micrometers and as finely dispersed calcite in the sub-micrometer range. Its Ca concentration shows variations between 63% (C-SL-2) and 70% (C-OPC). Layer OP at the surface of concrete is even more depleted in Ca than layer IP (Fig. 4). The Ca concentrations vary between 16% (C-OPC) and 28% (C-LS). Si is the main component with concentrations ranging from 39% (C-LS) to 55% (C-OPC). In general, sulphur content decreases approaching the surface, while the relative fractions of Al and Fe increase. The chemical gradients of Ca, S, Fe and Al are best shown in comparison with Si (Figs. 4 and 5).

3.4. Thermodynamic modeling

Thermodynamic modeling was used to calculate the changes associated in the different concretes in the presence of a solution with a water hardness of approx. 20 fH° and a pH of 7. In the calculations, only the interaction of the solution with the cement paste was considered, while no interaction with the aggregate was assumed. Concrete C-SL-1 with an intermediate cement composition between C-OPC and C-SL-2 was not modeled.

The unaffected core of concrete C-OPC is calculated to consist mainly of C–S–H, portlandite, ettringite and monocarbonate, with smaller quantities of calcite, hydrotalcite, and hemicarbonate (Fig. 6a). Upon the ingress of H_2CO_3 and $CaCO_3$ solution, the calculations predict that first portlandite becomes unstable and the Ca/Si ratio of the C–S–H starts to decrease (Fig. 6a). Eventually also the monocarbonate and ettringite become unstable forming calcite and small quantities of strätlingite. This leads to an inner zone which is leached with respect to calcium and sulphate. Nearer to the surface also the remaining C–S–H is leached to form calcite and amorphous silica gel. Note that the dissolution of amorphous SiO_2 gel was suppressed in the thermodynamic calculations as its dissolution kinetics is very slow at near neutral pH conditions.

The carbonate (and calcium) of the ingressing solution leads to the formation of a calcite layer in a zone where a calculated pH in the range of 8 to 12 is present (Fig. 7c). Additional calcium to form calcite is also leached from monocarbonate, ettringite and the C–S–H phase (Fig. 6). The formation of such a calcite layer fills up a significant portion of the available pore space. At the surface calcite is calculated to be unstable relative to the surrounding solution, while amorphous SiO_2, $Al(OH)_3$ and $Fe(OH)_3$ gel will persist. The outermost layer is depleted with respect to Ca and has a low degree of space filling (Fig. 7a and b). The calculated sequence of different layers agrees with the experimental observations in this study (see above Figs. 1–3). However, the calculated porosity in Fig. 7a corresponds to total porosity (sum of gel and capillary pores) and is higher than the volume of porous zones in the paste as determined by image analysis (Fig. 3 and Table 4).

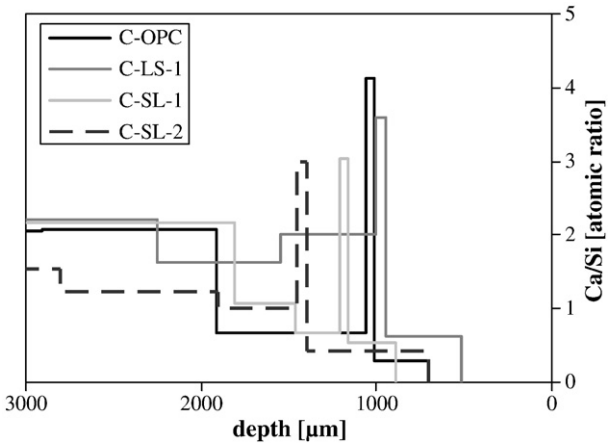

Fig. 4. Atomic ratio of Ca/Si present in the different layers of the four studied concrete mixtures.

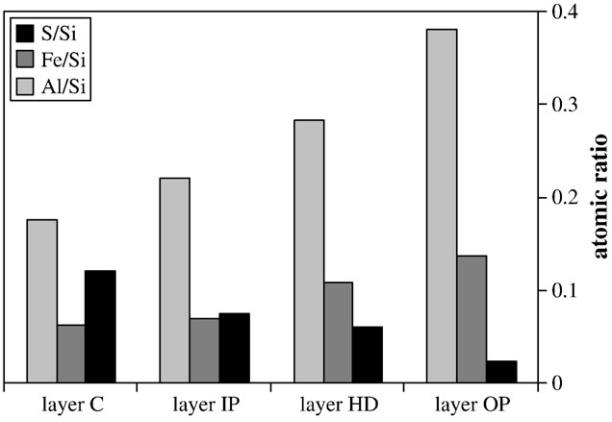

Fig. 5. Atomic ratio of S/Si, Fe/Si and Al/Si present in the different layers. Mean values of the four concrete mixtures.

The influence of H_2CO_3 and $CaCO_3$ solution on concrete C-LS is similar. The main difference to concrete C-OPC is the presence of additional calcite, which leads to slight dilution of Portland cement (Fig. 6b). The core region of concrete C-SL-2, which may contain up to 80% slag is calculated to consist of C–S–H (with a Ca/Si ratio of ~1.5), hydrotalcite, strätlingite and small amounts of monosulphate, mono- and hemicarbonate. The calculated changes associated with the ingress of calcium and carbonate containing solutions are similar to the changes in the other cements. Near the unaffected core, monocarbonate and ettringite become stabilized as carbonate ingresses. Eventually, both monocarbonate and ettringite become unstable with respect to calcite and strätlingite. Nearer to the surface, C–S–H and strätlingite convert to calcite, SiO_2 and $Al(OH)_3$. Significantly less calcite is calculated to be formed in concrete C-SL-2, as in its paste much less calcium is available which can react with carbonate to calcite (Fig. 6c). This leads to a smaller reduction of porosity in the calcite layer (Fig. 7a) and to lower buffer capacity against acidity as indicated by the lower pH values in the presence of concrete C-SL-2 (Fig. 7c).

Fig. 6. Calculated changes in the hydrate assemblage of a) concrete C-OPC (CEM I), b) concrete C-LS (CEM II/A-LL) and c) concrete C-SL-2 (CEM III/B) upon the ingress of a solution containing 0.67 mM $CaCO_3$ and 1.33 mM H_2CO_3. A complete reaction of the Portland cement clinker and a reaction degree of 50% of the slag in CEM III/B is assumed.

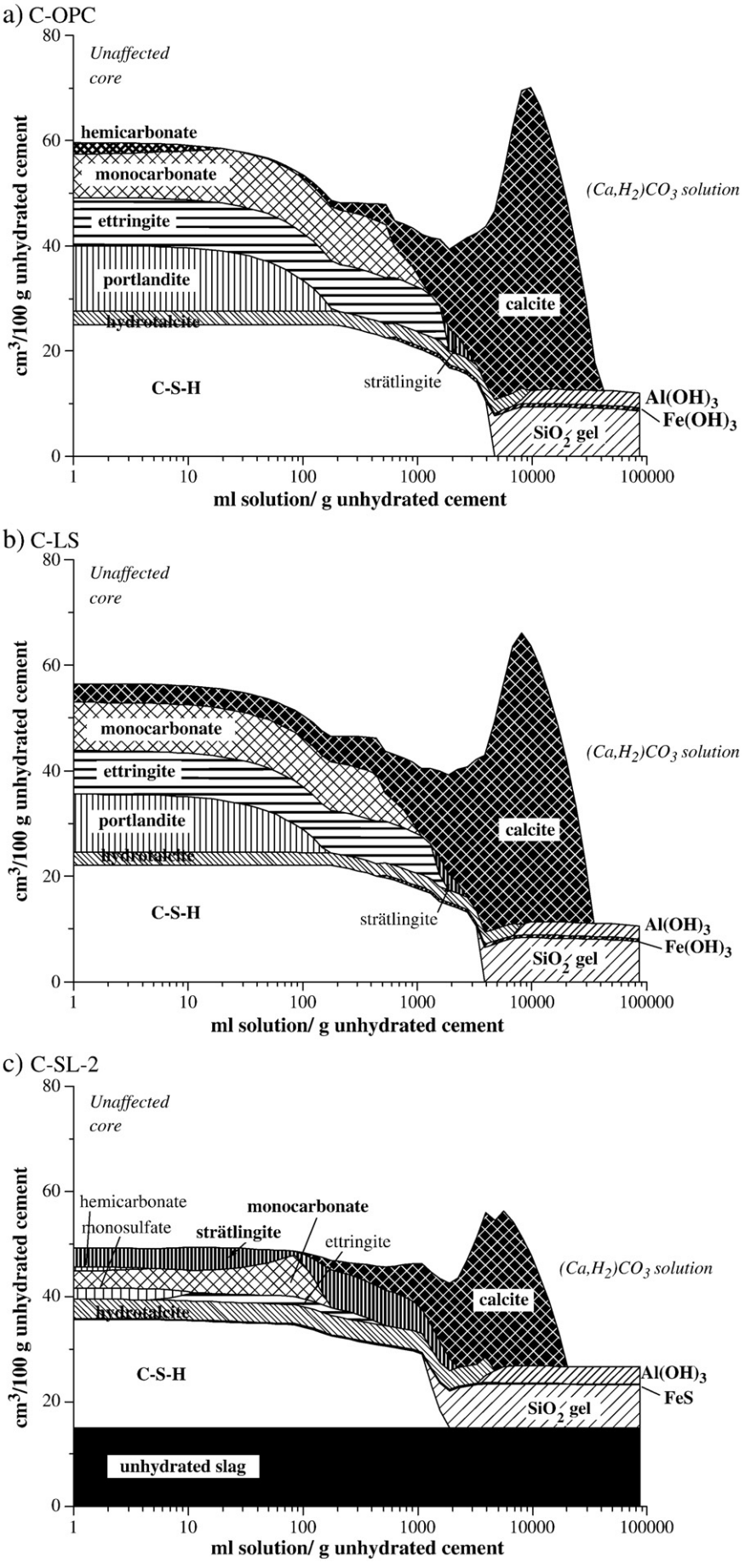
a) C-OPC
Unaffected core
hemicarbonate
monocarbonate
ettringite
portlandite
hydrotalcite
C-S-H
strätlingite
calcite
(Ca,H2)CO3 solution
Al(OH)3
Fe(OH)3
SiO2 gel
cm3/100 g unhydrated cement
ml solution/ g unhydrated cement
b) C-LS
Unaffected core
monocarbonate
ettringite
portlandite
hydrotalcite
C-S-H
strätlingite
calcite
(Ca,H2)CO3 solution
Al(OH)3
Fe(OH)3
SiO2 gel
cm3/100 g unhydrated cement
ml solution/ g unhydrated cement
c) C-SL-2
Unaffected core
hemicarbonate
monosulfate
monocarbonate
strätlingite
ettringite
hydrotalcite
C-S-H
calcite
(Ca,H2)CO3 solution
Al(OH)3
FeS
SiO2 gel
unhydrated slag
cm3/100 g unhydrated cement
ml solution/ g unhydrated cement

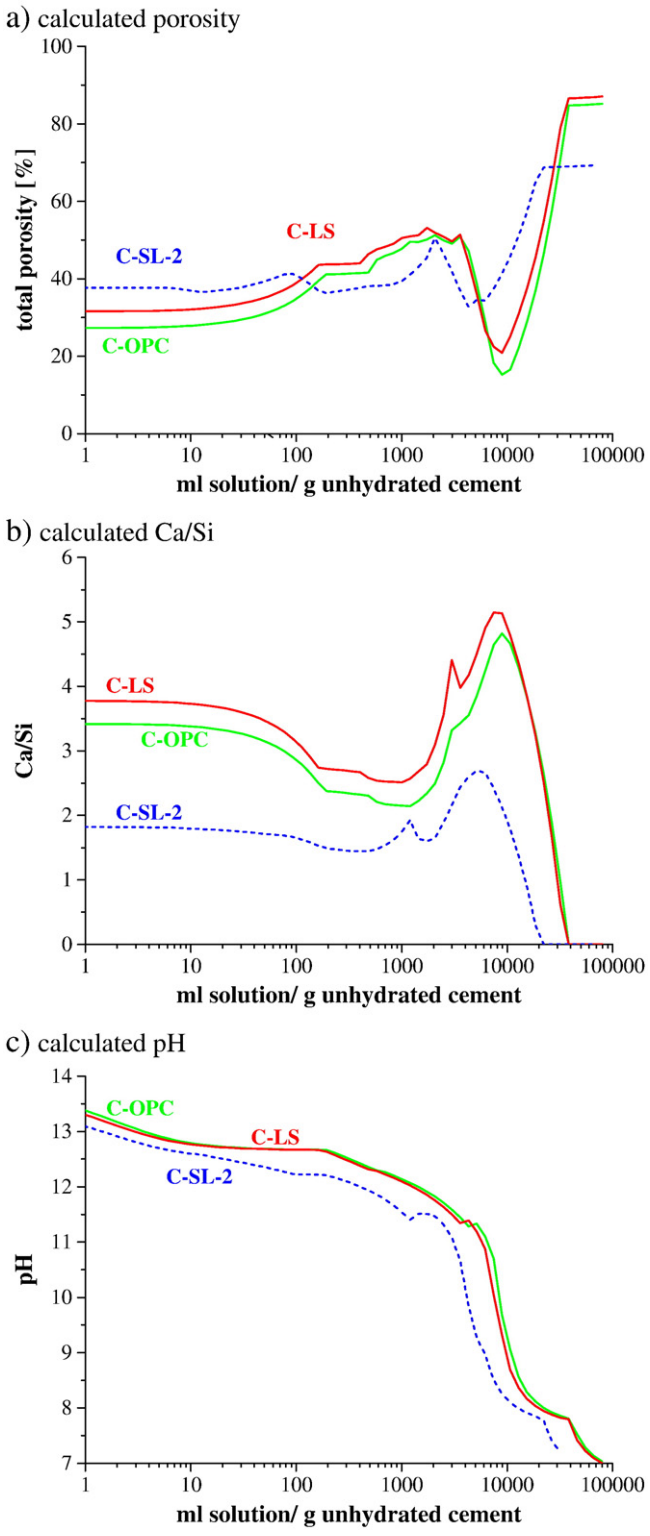

Fig. 7. Calculation for concretes C-OPC (CEM I), C-LS (CEM II/A-LL) and C-SL-2 (CEM III/B) a) total porosity of the concrete, b) molar Ca/Si ratio in the paste and c) pH in the pore solution upon the ingress of a solution containing 0.67 mM $CaCO_3$ and 1.33 mM H_2CO_3.

4. Discussion

The differences in oxygen diffusion between the different concrete mixtures are caused by the different cements, as w/c is identical. The presence of limestone powder as in concrete C-LS can increase porosity and permeability (Table 4, [35–37]). In contrast, the use of slag as in concrete C-SL-1 and C-SL-2 does not lower porosity but it lowers permeability due to smaller pore diameters (Table 4, [38,39]).

The changes in porosity observed in the different layers are caused by dissolution and precipitation of minerals. With progressing deterioration, portlandite is leached and C–S–H is decalcified as shown by the changes in Ca/Si ratio (layers IP and OP). The depletion of calcium at the concrete surface clearly indicates that the concrete corrodes due to an acid attack. However, the slow progress of deterioration indicates an only slightly acidic environment. The precipitation of calcite leading to the formation of layer HD occurs when the Ca ions react with the bicarbonate that is present in the attacking solution (Fig. 6, [20,40]). The concentration gradient of Ca in Fig. 4 shows, that Ca ions move towards the surface of the concrete. This observation makes it likely that at least a part of the Ca ions used to form layer HD origin from layer IP. The resulting formation of dense layer HD slows down further deterioration not only due to its low porosity but also because it acts as a buffer for the (slight) acidity of the intruding water [41]. The formation of a protective calcite layer has been observed in the presence of solutions containing calcium carbonates in oil well cements in the temperature range from 20 to 80 °C [40,42]. Furthermore, the formation of the surface layers increase the distance from the surface to the unaltered paste. Together with the low porosity of layer HD and its buffer capacity, they slow down the acid attack considerably. However, due to the high porosity of layers IP and OP, these surface layers exhibit low strength and may be easily removed by mechanical cleaning. Once the surface layers are removed, dissolution is increased again leading to a higher degree of deterioration [17,18,43]. Apart from calcium, the corroded zones are depleted in sulphur agreeing with the results obtained by leaching experiments of pastes with pure water [12,44]. Having a low solubility, the increase of Al and Fe towards the concrete surface is relative and an effect of Ca and S dissolution.

The depth of layer HD is a good marker of how far the attack has progressed into the concrete, and could be considered as a measure for the degree of biodeterioration [43].

The deterioration degree of the exposed cubes does not decrease with decreasing oxygen diffusion coefficient (Fig. 8) or with decreasing porosity of the unaffected core (Table 4). In fact, deterioration and oxygen diffusion coefficients of the unaltered concrete show an opposite trend. Even if concrete deterioration in the wastewater plant is a diffusion process, the initial diffusion coefficient is clearly not the governing parameter under the prevailing conditions. The comparison between the depth of layer HD and CaO content of the cements used for the different concrete mixtures uncovers that the latter is the main parameter controlling the process (Fig. 9). When the biofilm produces the same acidity on the surface of

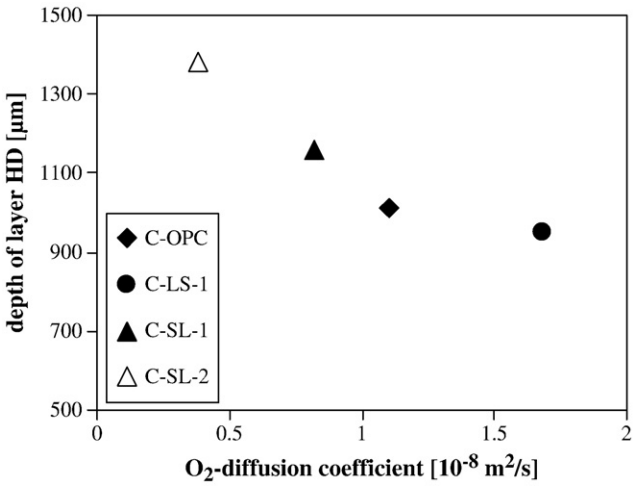

Fig. 8. Depth of calcite layer on untouched side versus oxygen diffusion coefficient.

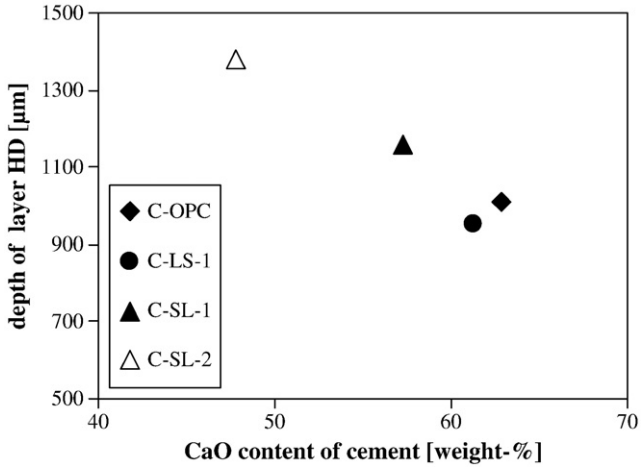

Fig. 9. Depth of calcite layer on untouched side versus CaO content of the cements used for concrete production.

the different mixtures, the buffer capacity of the individual concrete determines the volume of paste needed for neutralization or in other words the depth of deterioration. The presence of more CaO will lead to formation of more calcite resulting in greater decreases of porosity, which might even result in a complete blocking of the porosity as reported by Pfingsten et al. [41]. Even if this layer is generally thin, it will slow down diffusion. As the amount of CaO in the slag cements is lower than in OPC and cement with limestone powder, concrete C-SL-2 is affected the most and concrete C-OPC and C-LS the least. When a dense calcite layer is formed, it protects the concrete due to a decrease in diffusivity and due to its buffer capacity.

Diffusivity or permeability in the three degraded outer layers could not be determined experimentally. However, the diffusivity of cementitious materials produced with the same cement type depends on porosity (e.g. [45,46]). As an example, the porosity determined for concrete C-OPC (Table 4) can be used to assess relative diffusivity of the different surface layers according to Garboczi and Bentz [46]. The assessed values for layer HD are about 400 times lower than for layer OP and 70 times lower than for layer IP. Thus, even though layer HP is very thin, the transport of ions in the surface layers is slowed down significantly because of the formation of calcite in layer HD. Porosity in layer HD is comparable to the one in layer C.

The observed resistance of the different concrete mixtures does not agree with numerous leaching experiments using deionized water renewed in short intervals or with the resistance of concrete against strong acids that both show a higher resistance for systems with slag or fly ash compared to ordinary Portland cement systems [12,20–22,38,47,48]. In the first case, the absence of carbonates in the attacking solution prevents calcite precipitation and with it a densification of the microstructure [49]. A high CaO content of the cement and the presence of significant amounts of portlandite in the hydrated paste is even a disadvantage; portlandite dissolution increases diffusivity and accelerates the leaching process (e.g. [20]). In the second case, the low pH of the strong acids prevents calcite precipitation even when carbonates are present. In this case, the CaO content of the cement is insufficient to buffer the strong acids and the porosity created by portlandite dissolution leads also to a faster deterioration.

However, not only cement composition has to be taken into account assessing the deterioration resistance of concrete. Aggregate containing calcite should increase the buffer capacity of the concrete [38]. Especially the composition of the fines can be expected to be important due to their high surface area. A decrease of w/c can increase the resistance of the concrete [19–21]. The decrease of initial concrete diffusivity seems of minor importance in the present case. A low w/c leads to a higher density of the paste with an increase of CaO content per volume that should improve the buffer capacity of the concrete.

5. Conclusions

Concrete exposed in an aerated nitrification basin of a wastewater plant can be corroded due to proton production of a nitrifying biofilm covering it surface.

The deterioration caused in the acidic environment leads to specific microstructural features if significant quantities of bicarbonates are present in the water:

- layer OP: outer, highly porous layer depleted in calcium at the concrete surface
- layer HD: dense, calcite rich layer
- layer IP: layer with increased porosity compared to unaltered paste
- layer C: unaltered paste.

The formation of these layers and the increasing distance between biofilm/surface and unaltered paste slow down the rate of deterioration with time. Furthermore, layer HD slows down diffusion and acts as a buffer due to its low porosity and high calcite content.

The removal of these layers that offer some protection as often done in practice during cleaning accelerates deterioration.

The results of thermodynamic modeling show a good agreement with the experimental results and explain the observed profiles of porosity and chemical composition. Under the prevailing conditions, all concrete mixtures show surface deterioration. Its extent is not dependent on the diffusion coefficient of the unaltered concrete but on the CaO content of the cement used in the concrete. The presence of supplementary cementitious materials rich in Si and poor in Ca, such as slag, lowers the capacity to form calcite upon the ingress of carbonate containing solutions. If less calcite is formed, the porosity of the calcite rich layer HD should be higher and in addition the buffer capacity against the (slight) acidity of the intruding waste water is lowered. All these factors are expected to lower the resistance of cements with silicon rich mineral admixtures against slightly acidic solutions containing carbonates.

The influence of aggregate composition and w/c was not studied, but aggregates most likely influence the buffer capacity of the concrete, if they contain significant amounts of limestone. Furthermore, a low w/c should increase the resistance to deterioration as the higher density of the paste leads to a higher CaO content per volume of paste.

Acknowledgements

The authors would like to thank cemsuisse for financing this study and L. Brunetti and B. Ingold for the preparation of the polished samples.

References

[1] C.D. Parker, The corrosion of concrete 1. Isolation of a species of bacterium associated with the corrosion of concrete exposed to atmospheres containing hydrogen sulphide, Aust. J. Exp. Biol. Med. Sci. 23 (1945) 81–90.
[2] W. Sand, E. Bock, Biodeterioration of mineral materials by microorganisms — biogenic sulfuric and nitric acid corrosion of concrete and natural stone, Geomicrobiol. J. 9 (1991) 129–138.
[3] P.G. Jozsa, R. Stüven, E. Bock, M. Kussmaul, Statistical analysis of microbially influenced deterioration of concrete, Dechema-Monogr. 133 (1996) 199–208.
[4] W. Sand, Die Bedeutung der reduzierten Schwefelsäureverbindungen Schwefelwasserstoff, Thiosulfat und Methylmercaptan für die biogene SchwefelsaÈure-Korrosion durch Thiobacillen (The significance of sulfuric acid compounds like hydrogen sulfide, thiosulfate and methyl-mercaptane for sulfuric acid corrosion caused by Thiobacillus), Wasser Boden 5 (1987) 237–241.
[5] J.L. Davis, D. Nica, K. Shields, D.J. Roberts, Analysis of concrete from corroded sewer pipe, Int. Bioterior. Biodegrad. 42 (1998) 75–84.

[6] E. Vincke, N. Boon, W. Verstraete, Analysis of the microbial communities on corroded concrete sewer pipes — a case study, Appl. Microbiol. Biotechnol. 57 (2001) 776–785.
[7] W. Sand, Microbiological mechanisms of deterioration of inorganic substrates — a general mechanistic overview, Int. Biodeterior. Biodegrad. 40 (1997) 183–190.
[8] S. Okabe, H. Satoh, Y. Watanbe, In situ analysis of nitrifying biofilm as determined by in situ hybridization and the use of microelectrodes, Appl. Environ. Microbiol. 65 (1999) 3182–3191.
[9] H. Siegrist, W. Gujer, Demonstration of mass transfer and pH effects in a nitrifying biofilm, Wat. Res. 21 (1987) 1481–1487.
[10] P. Faucon, P. Le Bescop, F. Adenot, P. Bonville, J.F. Jacquinot, F. Pineau, B. Felix, Leaching of cement: study of the surface layer, Cem. Concr. Res. 26 (1996) 1707–1715.
[11] P. Faucon, F. Adenot, M. Jorda, R. Cabrillac, Behaviour of crystallized phases of Portland cement upon water attack, Mater. Struct. 30 (1997) 480–485.
[12] P. Faucon, F. Adenot, J.F. Jacquinot, J.C. Petit, R. Cabrillac, M. Jorda, Long-term behaviour of cement pastes used for nuclear waste disposal: review of physico-chemical mechanisms of water degradation, Cem. Concr. Res. 28 (1998) 847–857.
[13] M. Mainguy, C. Tognazzi, J.M. Torrenti, F. Adenot, Modelling of leaching in pure cement paste mortar, Cem. Concr. Res. 30 (2000) 83–90.
[14] K. Haga, M. Shibata, M. Hironaga, M. Tanaka, S. Nagasaki, Change in pore structure and composition of hardened cement paste during the process of dissolution, Cem. Concr. Res. 35 (2005) 943–950.
[15] K. Haga, S. Sutou, M. Hironaga, M. Tanaka, S. Nagasaki, Effects of porosity on leaching of Ca from hardened ordinary Portland cement paste, Cem. Concr. Res. 35 (2005) 1764–1775.
[16] [16] E. Koelliker, Über die Wirkung von Wasser und wässriger Kohlensäure auf Beton, Werkstoffwiss und Bausan, Int Koll, Esslingen, 1983.
[17] H. Grube, W. Rechenberg, Betonabtrag durch chemisch angreifende saure Wässer, Beton 11 (1987) 446–451.
[18] H. Grube, W. Rechenberg, Betonabtrag durch chemisch angreifende saure Wässer (Fortsetzung), Beton 12 (1987) 495–498.
[19] Y. Maltais, E. Samson, J. Marchand, Predicting the durability of Portland cement systems in aggressive environments — laboratory validation, Cem. Concr. Res. 34 (2004) 1579–1589.
[20] S. Kamali, M. Moranville, S. Leclercq, Material and environmental parameter effects on the leaching of cement pastes: experiments and modelling, Cem. Concr. Res. 38 (2008) 575–585.
[21] R.E. Beddoe, K. Schmidt, Effect of concrete composition on resistance of concrete to acid attack, in: Concrete in Aggressive Aqueous environments, M.G. Alexander, A. Bertron (Eds.), Proc Inter RILEM TC 211-PAE Final Conf, Toulouse, 2009, pp. 187–195.
[22] T.H. Wee, J. Zhu, H.T. Chua, S.F. Wong, Resistance of blended cement pastes to leaching in destilled water at ambient and higher temperatures, ACI Mater. J. 98 (2001) 184–193.
[23] S. Juretschko, G. Timmermann, M. Schmid, K.H. Schleiffer, A. Pommerening-Röser, H.P. Koops, M. Wagner, Combined molecular and conventional analysis of nitrifying bacterium diversity in activated sludge: *Nitrosococcus mobilis* and *Nitrospira*-like bacteria as dominant populations, Appl. Envir. Microbiol. 64 (1998) 3042–3051.
[24] Y. Aoi, T. Miyoshi, T. Okamoto, S. Tsuneda, A. Hirata, A. Kitayama, T. Nagamune, Microbial ecology of nitrifying bacteria in wastewater treatment process examined by fluorescence in situ hybridization, J. Biosci. Bioeng. 90 (2000) 234–240.
[25] H.B. Dionisi, A.C. Layton, G. Harms, I.R. Gregory, K.G. Robinson, G.S. Sayler, Quantification of *Nitrosomonas oligotropha*-like ammonia-oxidizing bacteria and *Nitrospira* spp. from full-scale wastewater treatment plants by competitive PCR, Appl. Environ. Microbiol. 68 (2002) 245–253.
[26] C.D. Lawrence, Transport of oxygen through concrete, in: F.P. Glasser (Ed.), The Chemistry and Chemically-related Properties of Cement, British Ceramic Soc. Proc., 35, 1984, pp. 277–293.
[27] D. Kulik, GEMS-PSI 2.2, available at http://gems.web.psi.ch/, PSI-Villigen, Switzerland, 2007.
[28] T. Thoenen, D. Kulik, Nagra/PSI chemical thermodynamic database 01/01 for the GEM-Selektor (V.2-PSI) geochemical modeling code, PSI, Villigen, 2003, available at http://gems.web.psi.ch/doc/pdf/TM-44-03-04-web.pdf.
[29] W. Hummel, U. Berner, E. Curti, F.J. Pearson, T. Thoenen, Nagra/PSI Chemical Thermodynamic Data Base 01/01, Universal Publishers/uPUBLISH.com, USA, 2002.
[30] B. Lothenbach, T. Matschei, G. Möschner, F.P. Glasser, Thermodynamic modeling of the effect of temperature on the hydration and porosity of Portland cement, Cem. Concr. Res. 38 (2008) 1–18.
[31] J.I. Escalante, et al., Reactivity of blast-furnace slag in Portland cement blends hydrated under different conditions, Cem. Concr. Res. 31 (2001) 1403–1409.
[32] J.S. Lumley, R.S. Gollop, G.K. Moir, H.F.W. Taylor, Degrees of reaction of slag in some blends with Portland cements, Cem. Concr. Res. 26 (1996) 139–151.
[33] B.R. Bickmore, K.L. Nagy, A.K. Gray, A.R. Brinkerhoff, The effect of $Al(OH)_4^-$ on the dissolution rate of quartz, Geochim. Cosmochim. Acta 70 (2006) 290–305.
[34] P.M. Dove, The dissolution kinetics of quartz in sodium chloride solutions at 25 degrees to 300 degrees C, Am. J. Sci. 294 (1994) 665–712.
[35] S. Tsivilis, J. Tsantilas, G. Kakali, E. Chaniotakis, A. Sakellariou, The permeability of Portland limestone cement concrete, Cem. Concr. Res. 33 (2003) 1465–1471.
[36] S. Tsivilis, E. Chaniotakis, G. Batis, C. Meletiou, V. Kasselouri, K. Kakali, A. Sakellariou, G. Pavlakis, C. Psimadas, The effect of clinker and limestone quality on the gas permeability, water absorption and pore structure of limestone cement concrete, Cem. Concr. Compos. 21 (1999) 139–146.
[37] T. Matschei, B. Lothenbach, F.P. Glasser, The role of calcium carbonate in cement hydration, Cem. Concr. Res. 37 (2007) 551–558.
[38] Z.T. Chang, X.J. Song, R. Munn, M. Marosszeky, Using limestone aggregates and different cements for enhancing resistance of concrete to sulphuric acid attack, Cem. Concr. Res. 35 (2005) 1486–1494.
[39] R. Loser, B. Lothenbach, A. Leemann, M. Tuchschmid, Chloride resistance of concrete and its binding capacity — comparison between experimental results and thermodynamic modeling, Cem. Concr. Compos. 32 (2010) 34–42.
[40] N. Neuville, E. Lecolier, G. Aouad, D. Damidot, Characterisation and modelling of physico-chemical degradation of cement-based materials used in oil wells, Proc Inter RILEM Symp Concr Modell — CONMOD'08', Delft (Netherlands), 2008, pp. 191–198.
[41] W. Pfingsten, Experimental and modeling indications for self-sealing of cementitious low- and intermediate-level waste repository by calcite precipitation, Nucl. Technol. 140 (2002) 63–82.
[42] A. Duguid, M. Radonjic, G. Scherer, The effect of carbonated brine on well cement used in geologic formations, 12th International Congress on the Chemistry of Cement, Montreal, Canada, TH4-10.2, 2007.
[43] A. Leemann, B. Lothenbach, C. Hoffmann, S. Bischof, P. Lunk, Concrete corrosion in a wastewater plant. In: Concrete in Aggressive Aqueous environments, in: M.G. Alexander, A. Bertron (Eds), Proc Inter RILEM TC 211-PAE Final Conf, Toulouse, 2009, pp. 116–124.
[44] M. Moranville, S. Kamali, E. Guillon, Physiochemical equilibria of cement-based materials in aggressive environments — experiment and modeling, Cem. Concr. Res. 34 (2004) 1569–1578.
[45] E.J. Garboczi, D.P. Bentz, Computer simulation of the diffusivity of cement-based materials, J. Mater. Sci. 27 (1992) 2083–2092.
[46] D.P. Bentz, E.J. Garboczi, Modelling the leaching of calcium hydroxide from cement paste: effects on pore space percolation and diffusivity, Mater. Struct. 25 (1992) 523–533.
[47] M.T. Bassuoni, M.L. Nehdi, Resistance of self-consolidation concrete to sulfuric acid attack with consecutive pH reduction, Cem. Concr. Res. 37 (2007) 1070–1084.
[48] E. Gruyaert, N. De Belie, P. Van den Heede, Acid resistance of concrete containing blast-furnace slag: influence of the pore structure and hydration process, in: Concrete in Aggressive Aqueous environments, M.G. Alexander, A. Bertron, (Eds.), Proc Inter RILEM TC 211-PAE Final Conf, Toulouse, 2009, pp. 389–396.
[49] A. Leemann, B. Lothenbach, H. Siegrist, C. Hoffmann, Influence of water hardness on concrete surface deterioration caused by nitrifying biofilms in waste water treatment plants, Int. Biodeterior. Biodegrad, accepted.